This is the author's manuscript draft version of the contribution published as:

Kamjunke, N., Hertkorn, N., Harir, M., Schmitt-Kopplin, P., Griebler, C., **Brauns, M.**, **von Tümpling, W.**, **Weitere, M.**, **Herzsprung, P.** (2019):
Molecular change of dissolved organic matter and patterns of bacterial activity in a stream along a land-use gradient
Water Res. **164** , art. 114919

The publisher's version is available at:

http://dx.doi.org/10.1016/j.watres.2019.114919

Molecular change of dissolved organic matter and patterns of bacterial activity in a stream along a land-use gradient

Norbert Kamjunke[1]*†, Norbert Hertkorn[2†], Mourad Harir[2,3], Philippe Schmitt-Kopplin[2,3], Christian Griebler[4,5], Mario Brauns[1], Wolf von Tümpling[1], Markus Weitere[1], Peter Herzsprung[6†]

[1]Helmholtz-Centre for Environmental Research - UFZ, Department of River Ecology, Brückstraße 3a, D-39114 Magdeburg, Germany

[2]Helmholtz-Centre Munich, German Research Center for Environmental Health, Research Unit Analytical Biogeochemistry (BGC), Ingolstädter Landstraße 1, P. O. Box 1129, D-85758 Neuherberg, Germany

[3]Technical University Munich, Chair Analytical Food Chemistry, Maximus-von-Imhof-Forum 2, D-85354 Freising Weihenstephan, Germany

[4]Helmholtz-Centre Munich, German Research Center for Environmental Health, Institute of Groundwater Hydrology (IGOE), Ingolstädter Landstraße 1, P. O. Box 1129, D-85758 Neuherberg, Germany

[5]Present address: University of Vienna, Department of Limnology & Bio-Oceanography, Althanstrasse 14, 1090 Vienna, Austria

[6]Helmholtz-Centre for Environmental Research - UFZ, Department of Lake Research, Brückstraße 3a, D-39114 Magdeburg, Germany

*corresponding author: Tel.: +49 391 8109434, fax: +49 391 8109150, e-mail: norbert.kamjunke@ufz.de

[†]These authors contributed equally to the manuscript.

Key words: DOM; FTICR MS; NMR; stream; WWTP; bacterial production; biofilm

Abstract

Fluvial networks are globally relevant for the processing of dissolved organic matter (DOM). To investigate the change in molecular DOM diversity along the river course, high-field FTICR mass spectrometry and NMR spectroscopy of riverine DOM as well as bacterial abundance and activity were measured in a third order stream along a land-use gradient from pristine, agricultural to urban landscapes. DOM composition showed a clear evolution along the river course with an initial decrease of average oxidation and unsaturation followed by an increased relative abundance of CHNO and CHOS compounds introduced by agriculture and waste water, respectively. DOM composition was dominated by rather unsaturated CHO compounds (H/C $\leq$1) in headwaters and by more aliphatic molecules at downstream sites. Oxygenated functional groups shifted from aromatic ethers and hydroxyl groups to aliphatic carboxylic acids and aliphatic hydroxyl groups. This massive dislocation of oxygen significantly increased the diversity of atomic environments in branched aliphatic groups from headwater to downstream DOM. Mass spectra of DOM enabled the detection of compositional relationships to bacterial abundance and activity which was positively related to more aliphatic components (H/C >1) and negatively related to unsaturated components. FTICR mass and NMR spectra corroborated the initial decline in DOM molecular diversity predicted by the River Continuum Concept (RCC) but demonstrated an anthropogenic increase in the molecular diversity of DOM further downstream. While the high DOM molecular diversity in first order headwater streams was the result of small scale ecosystem plurality, agriculture and waste water treatment introduced many components in the lower reaches. These anthropogenic influences together with massive bacterial oxidation of DOM contributed to a growth of molecular diversity of downstream DOM whose composition and structure differed entirely from those found in pristine headwaters.

1. Introduction

Streams and rivers are important sites for organic carbon processing. They receive considerable amounts of terrestrial organic matter (Aufdenkampe et al. 2011) of which a large proportion is humic-like aromatic-rich material dominated by lignin and tannin compounds (Mosher et al., 2015). Along the river course from mountain springs and headwaters to the lowlands, algal photosynthesis contributes to increasing proportions of autochthonous DOM (Jaffe et al., 2012; Parr et al., 2015). The river continuum concept predicts a high molecular diversity of DOM in first order streams with high proportions of groundwater DOM and decreasing diversity in second order to fifth order streams (Vannote et al. 1980). On the other hand, rivers receive molecules from anthropogenic sources such as agriculture, industry, and waste water treatment (Hosen et al., 2014; Parr et al., 2015) contributing to the overall molecular diversity of DOM. Thus, it is very likely that the molecular diversity of riverine DOM will evolve along the river course and might in fact increase from the source to the confluence with higher order streams.

DOM quality and its changes in streams are commonly assessed using fluorescence spectra (Cory and Kaplan, 2012; Hosen et al., 2014; Parr et al., 2015). Several indices relating specific excitation and emission wavelengths were developed, e.g. an increased freshness index (Fellmann et al., 2010) indicates more microbially produced DOM and a decreased humification index (Zsolnay, 2003) indicates less plant-derived DOM due to farming which increased also dissolved organic nitrogen concentration (Graeber et al., 2015). In urban streams, the proportion of humic-like allochthonous DOM was lower whereas the more bioavailable autochthonous DOM showed higher proportions (Parr et al., 2015).

Fourier transform ion cyclotron resonance mass spectrometry (FTICR MS) detects gas phase ions of molecules with very high molecular resolution enabling the assignment of thousands of CHO, CHNO, CHOS and CHNOS molecular formulas (Hertkorn et al., 2008). However it is subject to ionization selectivity, and many isomeric molecules may project on any

77 individual mass peak. NMR spectroscopy allows the analysis and quantification of carbon-
78 and hydrogen-based aliphatic, oxygenated and aromatic chemical environments of atoms.
79 Together, FTICR and NMR mass spectra provide complementary information about structure
80 and molecular composition of DOM (Hertkorn et al., 2007). While in recent years, several
81 mass spectrometry based studies of riverine DOM were performed at single sites of one or
82 more streams (Kim et al., 2006; Stubbins et al., 2010; Sleighter et al., 2014; Wagner et al.,
83 2015), only a single study (Mosher et al., 2015) covered a longitudinal transect from
84 headwater streams proceeding downstream. To the best of our knowledge, no nuclear
85 magnetic resonance spectroscopy (NMR) analysis covers evolution of riverine DOM along
86 the river course.
87 Biological processing of DOM in streams and rivers is mainly performed by heterotrophic
88 bacteria and leads to breakdown of large molecule and ultimate CO_2 emissions from running
89 waters while other fractions of DOM might flocculate and become part of sedimentary carbon
90 or are exported to the ocean (Cole et al., 2007; Battin et al., 2008; Hale and Godsey, 2019).
91 This processing can be performed by planktonic, suspended stream water bacteria or by
92 epilithic bacteria associated in biofilms (Battin et al., 2003, 2008). Previous studies have
93 shown that the activity of planktonic bacteria was related to DOM quality while activity of
94 biofilm bacteria was not due to benthic algae and extracellular polymeric substances as
95 additional carbon sources in biofilms (Kamjunke et al., 2015). However, bacterial activity was
96 only related to bulk optical parameters and could not be related to specific carbon species so
97 far. Here we tested the hypotheses that (1) DOM diversity decreases along the river course,
98 and (2) bacterial abundance and activity are related to specific DOM components. This
99 research requires a highly resolved molecular DOM-characterization not commonly available.
100 In this contribution we related FTICR MS- and NMR-based, better constrained molecular
101 composition and structure of riverine DOM to biological processing along a representative
102 German third order stream with a land-use gradient ranging from pristine headwaters with

forest catchment, through a variety of urban and agricultural areas with well documented land use (Wollschläger et al., 2017).

2. Material and Methods

2.1. Study area and sampling

The study was done in the Holtemme catchment area in the Harz Mountains, Germany which is part of an observation network called Terrestrial Environmental Observatories (TERENO; Wollschläger et al., 2017). The Holtemme River is a third order river in the Elbe catchment area with a long-term mean annual discharge of 1.34 $m^3 s^{-1}$ (gauging station Mahndorf) that originates at 862 m a.s.l. and flows into the Bode River. The land use in the catchment is dominated by agriculture (60%), followed by forests (30%) and urban (10%) areas (Wollschläger et al., 2017). The hydromorphology is natural in the upstream sections but highly impacted due to channeling, riparian clearcutting and incision in urban and agricultural areas. The river receives substantial pollution from two wastewater treatment facilities serving a population equivalent of more than 40,000 each and from tributaries draining agricultural areas. Sampling of DOM quality and bacteria was performed at 12 sites from headwater to the mouth (Fig. 1, Table S1) on 6th and 7th October 2014 under base flow conditions as DOM is controlled by instream processes during the late growing season but by transport during high flow (Hale and Godsey, 2019).

2.2. Measurement of DOC concentration and fluorescence

DOC concentrations were determined after high-temperature combustion (DIMATOC 2000, Dimatec Analysentechnik GmbH, Essen, Germany). Fluorescence excitation emission matrices (EEMs) were collected using a spectrofluorometer (AQUALOG, HORIBA Jobin Yvon, USA; see SI for details).

2.3. High-field FTICR mass spectrometry of DOM

2.3.1. Solid phase extraction (SPE), FTICR mass spectra determination

Aliquots of 70 mL water were filtered through pre-combusted GF/F and acidified with HCl to pH 2.0. Subsamples of 50 mL of the acidified filtrate were processed through 500 mg styrene-divinyl-polymere type (PPL) solid-phase cartridges (Agilent, Waldbronn, Germany) prior to electrospray ionization (ESI) using a SmartPrep® automatic cartridge extractor (Horizon Technology, Salem, USA). The SPE-DOM was extracted twice with 2 mL methanol; the extracts were diluted with methanol to 5 mL and were stored at -20°C until analysis (Dittmar et al., 2008; Raeke et al., 2016). The recovery rates of the 12 samples are shown in Table S2. The details of FTICR MS measurements (electrospray ionization in negative mode) were described in Hertkorn et al. (2016), Herzsprung et al. (2017), and the SI.

2.3.2. Analysis based on ranks of intensities of single components

Hierarchical cluster analysis (HCA) was performed with STATISTICA 12 software by Statsoft® using the calculated intensity ranks (Herzsprung et al., 2017). The rank correlations were performed on the basis the calculated inter sample ranks of the molecular compositions which were present in all 12 samples (n = 749; see SI for details).

2.3.3. Analysis based on normalization of mass peak intensities of single components

The relative mass peak intensities (n = 4616, all different components with present counts between 1 and 12) were obtained from intensity-normalized mass spectra (Osterholz et al., 2016; Kamjunke et al., 2017). This procedure was applied to each of the 12 samples and was used to evaluate longitudinal DOM quality changes. We applied a linear regression between the relative mass peak intensity as dependent variable and the distance of the sampling sites from the source where the slope was regarded as semi-quantitative parameter for the change: A positive/negative slope basically means an increase/decrease of the component abundance along the flow length. For visualization in van Krevelen diagrams we used only components which were present in at least 8 samples and with $p < 0.05$ ($R^2 > 0.332$).

155

156 *2.4. NMR spectroscopy of SPE-DOM*

157 Proton-detected NMR spectra of methanolic riverine SPE-DOM extracts were acquired using
158 a Bruker Avance III NMR spectrometer at 800.13 MHz (B_0 = 18.7 T) and 283 K from ~1 mg
159 of solid SPE-DOM obtained by evaporation of the original methanol-h_4 solution (for details
160 see SI).

161

162 *2.5. Bacterial abundance and biomass production*

163 Abundance of planktonic bacteria from formalin-fixed samples and of biofilm bacteria after
164 detachment by ultrasonication was estimated after staining with acridine orange and counting
165 using an epifluorescence microscope (Axioskop2, Zeiss) according to Kamjunke *et al.* (2015).
166 Production of planktonic and epilithic biofilm bacteria was measured using the leucine
167 technique (Simon and Azam, 1989) as described by Kamjunke et al. (2015) after storage of
168 samples at 4°C until the next day (see SI for details). The assimilable organic carbon (AOC)
169 was estimated from the growth of bacterial cells in a dilution batch experiment running for 30
170 days at ambient temperature (15°C) in the dark (see SI for details). We applied Spearman
171 rank correlations between bacterial abundance, BP, cell-specific BP, and AOC with DOM
172 fluorescence indices, intersample ranks of FTICR MS components present in all samples, and
173 ^{1}H NMRsection integrals (Herzsprung et al., 2017). For components introduced by the input
174 from diverse sources (i.e. which were not present in all samples), we performed Spearman
175 correlations for linked (equal) values (Sachs, 1974) with the intersample ranked intensities
176 (Herzsprung et al., 2012) which were present in at least 7 samples and with $p < 0.05$ ($R^2 >$
177 0.332).

178

179 **3. Results**

180 *3.1. Bulk parameter analysis*

Discharge increased continuously from the source to site 6 which might be explained by the inflow of several tributaries and the effluent of the first WWTP (Fig. 2). Further downstream, discharge remained nearly constant with low contributions of tributaries. DOC concentrations were highest in the headwater section and decreased from site 1 to site 4, partly due to dilution by tributaries with lower DOC concentration. From there, the DOC was nearly constant at a level of about 3 mg L^{-1}. Fluorescence and freshness index increased slightly until site 4, showed a steep increase in response to the first WWTP, and remained constant afterwards. Humification index and specific UV absorption decreased until site 5 and did not change further downstream. FTICR mass spectra showed clear changes along its river course. SPE-DOM from sites 1 and 2 showed skewed, near Gaussian type distributions of mass peaks with a steeper slope toward lower mass ($m/z < 350$) than toward higher mass ($m/z > 450$; Fig. S1). Overall mass peak distributions became more symmetrical downstream. From site 3 downstream, various groups of sharp mass peaks indicated restricted sets of abundant molecules. At sites 4 and 5, patterning indicated presence of either abundant biomolecules from DOM processing or anthropogenic compounds. From site 7 downwards, a distinct group of low mass peaks ($m/z < 300$) appeared. The average H/C ratio indicated a transition from more unsaturated (sites 1-3) toward more saturated aliphatic molecules at sites 4-12 whereas the O/C ratio decreased from sites 2-5. The O/C ratio slightly increases from site 5 – 7 and decreased in response to the second WWTP again (where H/C increased in parallel; Fig. 2). The average oxidation state of carbon OS_C as well as the average mass continually declined from site 2 until sample 5 (after WWTP 1) and showed similar behaviour as the O/C ratio.

3.2. Classification and inter sample ranking

The hierarchical cluster analysis (HCA) computed from FTMS-derived molecular compositions which were present at all 12 sites (Fig. S1B) showed that the DOM quality in the headwater up to site 3 was completely different from the DOM quality in the lower

course. Sites 4 – 7 were rather similar among themselves, with sites 4/5 and 6/7 most likewise, whereas sites 8-12 were even more alike, with site 9 slightly dissimilar. The inter-sample rankings analysis projected on van Krevelen diagrams revealed more specific differences in DOM quality (Fig. 3). The headwater sites 1 – 3 showed mainly 1^{st} to 4^{th} ranks for O-rich polyphenol-like and highly unsaturated (O-rich; $H/C \leq 1$) components (van Krevelen coordinates shown in Fig. S4, according to Rossel et al., 2017), in the following combined and named as O-rich&DBE-richComp (Herzsprung et al., 2012). and 9^{th} to 12^{th} ranks for more aliphatic and oxygen-poor components ($O/C < 0.5$ and $H/C > 1$) and some oxygen-rich components with $H/C > 1$. The samples from sites 4 – 7 showed middle ranks for O-rich&DBE-richComp (3^{th} to 8^{th}) whereas the downstream sites 8 - 12 showed 7^{th} to 12^{th} ranks for these components. Overall, higher ranks shifted from O-rich&DBE-richComptoward higher aliphaticity (H/C ratio) and less oxygenation (O/C ratio) along the river course of Holtemme.

3.3 Analysis of the slope of FTICR mass peak intensities along the Holtemme river course

The evolution of molecular compositions along the river course was deduced from changes in relative mass peak intensity versus distance from Holtemme origin; an example plot (Fig. S5A) covers five representative molecular compositions (three CHO and one CHOS/CHNO molecules each). The slopes were visualized according to CHO, CHNO, and CHOS compounds (Fig. 4A). The relative intensity of O-rich&DBE-richComp decreased considerably (Fig. 4A, section b) along the Holtemme River whereas compounds of near average unsaturation and oxygenation increased in relative abundance (Fig. 4A, section a). CHNO of overall smaller chemodiversity than CHO compounds ($0.8 < H/C < 1.3$; $0.4 < O/C < 0.7$) near continually increased along the Holtemme River (Fig. 4A, section c). While the majority of CHOS components showed higher extent of oxygenation but near identical relative unsaturation ($1 < H/C < 1.7$; $0.4 < O/C < 0.8$) than respective CHO compounds (Fig.

4A, section e), three characteristic CH_2-based homologous series of CHOS components strongly increased downstream (Fig. 4A, section d; Table S6).

The distinct evolution of DOM molecular compositions downstream was visualized by recognizing only molecular compositions which *first appeared* at the specific sampling points 2-11 (any composition in site 1 is "new" by definition) *and then remained abundant* in *all* consecutive sampling points downstream (Fig. 4B). The presence of new components (mainly CHOS) was first observed at site 5 as response to WWTP1. At site 6, the highest number of new components was detected. The 153 components which were absent in samples 1-5 and present in samples 6-12 are shown in an additional van-Krevelen diagram (insert). A suite of CHNO compounds showed considerable oxygenation and unsaturation. In the last downstream sample from site 12, the many new appearing components represent an inevitable artefact of the *last* sampling point; analogous low intensity components are exclusively observed in any sample but not present in other samples (Riedel and Dittmar, 2014). Components with the lowest percentage intensity values are not far from signal to noise ratio. Components present in all samples had the highest intensities whereas components present in only one sample had comparably low intensities (Table S7).

The overall count of molecular compositions uniformly declined from site 1, reaching a minimum count at site 4 to grow again to site 6, to then stay nearly constant (Fig. 4c). The proportions of molecular series also changed: the relative abundance of CHO compounds declined nearly continually from source to outflow whereas the relative proportion of non-oxygen heteroatom-containing molecules grew in the order CHNOS < CHNO < CHOS compounds, with a decisive onset from site 4 (Fig. S2). While the average C/N ratio levelled off from site 6, the C/S ratio more gradually declined along the river course (Table S5). With recognition of the sharp increase in abundance of CHNO, CHOS and CHNOS compounds from site 6 downstream (Fig. 4c), another HCA was computed based solely on these molecular compositions which were present in all samples from site 6 to site 12 (Fig. S3).

Here, samples from sites 6 and 7 were quite similar while all remaining samples (8 – 12) clustered distinctly. The attendant van Krevelen diagram showed that these compounds were of average oxygenation and fairly unsaturated; the relative unsaturation as expressed by the average H/C ratio and the overall chemodiversity declined in the order CHOS > CHNO ~ CHNOS components.

Group-specific results showed a decrease of O-rich&DBE-richComp from sample 1 – 5 (Fig. 5a). The group highly unsaturated O-poor componentsand the group highly unsaturated O-rich ($1 < H/C < 1.5$) both increased from sample 1-4, the first one increased further to sample 5 but the latter one decreased from sample 4 – 5. Regarding CHOS components, all components with steep increases along the lines d_1, d_2 and d_3 in Fig. 4A were not detectable between sites 1-4. They increased steeply after the first WWTP, decreased at sites 6 and 7 (except for $C_{17}H_{26}O_5S$), and showed a strong increase again downstream the second WWTP. CHNO and CHNOS showed mainly different behaviour to the d_1, d_2 and d_3 CHOS (Fig. S6).

3.4 ^{1}H NMR spectra

All ^{1}H NMR spectra of Holtemme SPE-DOM from sites 1-12 showed broad superimposed NMR resonances typical of a fairly processed riverine organic matter. However, groups of relatively sharp aliphatic and aromatic NMR resonances indicative of rather early stages of DOM processing were more abundant in the upstream region. All SPE-DOM featured a high aliphaticity with a substantial proportion of open chain aliphatic carboxylic acids (cf. below). The evolution of the ^{1}H NMR section integrals along the river course appeared inconspicuous (Table S7): a rather marginal decline of purely aliphatic units (CCC**H**) was compensated to a minor extent by an increased abundance of functionalized aliphatics (OCC**H**) while oxygenated aliphatic units (OC**H**) remained nearly constant (Fig. S9; Table S9).

HCA and PCA resulted in a clear distinction of sites from sites 1 and 2 against all other samples (Fig. S10), while the further evolution of DOM along the river course was not

285 governed by a straight process. The distinction of SPE-DOM 1 probably reflected genuine
286 contributions from natural input of phenolic- and lignin-rich materials from a pristine forest
287 environment which also caused an elaborate and abundant array of OCH_3 groups (Table S9;
288 Fig. S11a; Fig. S12). SPE-DOM 2 was dominated by a uniquely abundant and rather specific
289 lipid-like component resonating at the positions δ_H ~ 0.90, 1.24-1.35, 1.55-1.63, 2.03 and 2.17
290 ppm which showed resolved J-couplings. This is indicative that these distinct NMR features
291 arose from only a few compounds. These abundant lipid-like components relatively
292 attenuated the amplitude of all other background NMR resonances typical for natural organic
293 matter which reflected a higher diversity of directly (OC**H**) and remotely (OC_n**H**; $n \geq 2$)
294 oxygenated aliphatic branching motifs in general. A direct comparison of SPE-DOM from
295 sites 1 and 2 (Fig. S12) demonstrated that apart from the unique set of lipid-like compounds,
296 the section of common NOM molecules was far less oxygenated at site 2 than at site 1 while
297 still showing an appreciable diversity of aliphatic branching motifs (Hertkorn et al., 2015).
298 Values of ^{1}H NMR section integrals with 0.01 ppm resolution were related to the river
299 distance of the 12 sites (see Fig. S5B for five examples) resulting in a slope over the river
300 stretch for each integral. A comparison of area-normalized ^{1}H NMR spectra at full resolution
301 revealed significant trends of DOM structure-chemical evolution along the river course which
302 were not available from ^{1}H NMR section integrals (Fig. 6). In summary, open chain aliphatics
303 of a limited structural diversity which comprised mainly variants of HOOC-CH_α-CH_β-CH_γ-
304 CH_δ…CH_3 units produced groups of relatively sharp NMR resonances which were more
305 abundant in the headwaters than downstream. These hugely superimposed NMR resonances
306 were caused by a mixture of many open-chain branched aliphatic carboxylic acids and
307 resonated at rather specific positions [$\delta_H(CH_\alpha)$ ~ 2.1-2.4 ppm; $\delta_H(CH_\beta)$ ~ 1.6 ppm; $\delta_H(CH_\gamma)$ ~
308 1.35 ppm; δ_H ($CH_{\delta,\varepsilon}$) ~ 1.3 ppm; $\delta_H(CH_3)$ ~ 0.89 ppm] (Hertkorn et al., 2015). These
309 prominent NMR resonances became gradually attenuated while broad NMR resonances
310 ranging from δ_H ~ 0.9 – 2.8 ppm and 3.4-4.3 ppm near continually grew in abundance when

311 proceeding downstream from source to mouth (Fig. 6C; Fig. S11a,b). These broad NMR
312 resonances represented an enormous diversity of aliphatic compounds with alicyclic rings
313 (Meckenstock et al., 2014) and remote oxygen substitution (OC_n**H**; n > 2) at δ_H ~ 0.9-2.0 ppm
314 (Fig. S11a,b), HOOC-C**H**α- units characteristic of carboxyl-rich alicyclic molecules (CRAM;
315 Hertkorn et al., 2006) and other carboxylic acids at δ_H ~ 2.2-2.8 ppm, and oxygenated
316 aliphatic units (OC**H**) at δ_H ~ 3.3-4.8 ppm (Fig. S11a,b).
317
318 *3.5 Bacterial abundance and production and their correlation to DOM quality*
319 The abundance of planktonic bacteria started with low values in headwaters, showed a first
320 increase between sites 4-5, and a larger increase between sites 7-8 (Fig. 7). Planktonic BP was
321 lowest in the headwaters of Holtemme (sites 1 and 2) and increased at sites 3, 5 and 9, the
322 cell-specific BP was highest at site 3 and decreased downstream. The longitudinal variability
323 of biofilm bacterial abundance was lower than that of planktonic bacteria with a maximum
324 value at site 5.The longitudinal dynamics of biofilm BP and cell-specific biofilm BP was not
325 very pronounced. The assimilable organic carbon ranged from 0.02 to 0.2 mg C L^{-1} and
326 showed particularly high values at sites 5 and 10. Abundance and BP of planktonic bacteria
327 were positively related to fluorescence and freshness index of DOM and negatively to
328 humification index and SUVA whereas no relationships were found for cell-specific BP
329 (Table S10). Biofilm abundance and BP as well as AOC did not correlate to DOM
330 fluorescence. Planktonic abundance showed very strong positive correlations to FTICR MS
331 components with low O/C and high H/C ratios and very strong negative correlations to
332 components with high O/C and low H/C ratios (Fig. 8). Planktonic BP was less strongly
333 related to these groups, and cell-specific BP showed only few significant correlations (Fig.
334 S15). Biofilm abundance and BP showed few specific positive relationships to components
335 with H/C ≥ 1 and different O/C and negative ones to components with H/C < 1 and O/C < 0.5.
336 The AOC was negatively related to very few components. The Spearman correlations

considering components present at at least 7 sites were also strongest for planktonic abundance and BP for CHO, CHNO, and particularly CHOS components whereas correlations to biofilm BP were moderate and to biofilm abundance and AOC were weaker (Fig. S14a-c). Parameters of bacterial abundance and activity were also correlated to section integrals of ^{1}H NMR spectra (Fig. 9). Planktonic abundance and BP were mainly positively related, particularly at δ_H ~1.0-5.0 ppm and δ_H ~6.5-9.0 ppm. Biofilm abundance and BP showed positive rank correlation coefficients at δ_H ~1.0-2.8 ppm and δ_H ~6.5-8.0 ppm. In contrast, AOC showed mainly negative rank correlation coefficients.

4. Discussion

Insights in DOM dynamics from bulk optical parameters and elemental composition

Several studies investigated the effect of agricultural land use on DOM quality in rivers by measuring its optical properties. Usually, the humification index (HIX) as a measure of terrestrial DOM decreased and the freshness index (β/α) as a measure of autochthonous DOM increased with an increase of agriculture in the catchment (Graeber et al., 2015). As a consequence of changing DOM quality, the partial pressure of CO_2 in water was higher in agricultural streams compared to forest streams, it was negatively correlated to molecular size and allochthonous DOM (Kamjunke et al., 2013; Bodmer et al., 2016). In the Holtemme River, DOC concentration was highest in the headwaters and remained rather constant after an initial decrease. The humification index decreased by a factor of three from forest to agricultural catchments whereas the freshness index doubled along that reach which is typical in streams (e.g., Williams et al., 2010; Kamjunke et al. 2015; Ejarque et al., 2017).

Joint analyses using structural and optical properties of DOM in combination were recently applied to investigate DOM quality with molecular resolution (Lavonen et al., 2015; Hertkorn et al., 2016; Herzsprung et al., 2017) and we also correlated fluorescence indices and FTICR MS results for the Holtemme (e.g., positive correlation between O-rich&DBE-richComp and

363 HIX and SUVA; Fig. S8). We observed O-rich&DBE-richComp (Fig. 3) with high molecular
364 weight (Table S4) in headwaters of the Holtemme which were found also for soil organic
365 matter at forested sites (Seifert et al., 2016). The relative abundances of O-rich&DBE-
366 richComp decreased downstream in the Holtemme. The high upstream concentrations, which
367 are confirmed by high HIX values, might be explained by the large proportion of forests and
368 wetlands in the upper catchment which are usually a source of such highly oxygen-rich and
369 aromatic components. The decrease of O-rich&DBE-richComp concentrations downstream
370 had four potential causes: photodegradation (Stubbins et al., 2010; Riedel et al., 2016),
371 dilution, precipitation with iron minerals (Dadi et al., 2017), and mixing with a tributary
372 containing different DOM quality. Biodegradation of O-rich&DBE-richComp is less
373 important in these fast flowing cold headwaters as these components are assumed to be
374 relatively recalcitrant in the dark (Riedel et al., 2016) whereas dilution play a role in the
375 upstream part of Holtemme (Fig. 2).
376
377 *Process analyses by combination of structural information and elemental composition*
378 ^{1}H NMR spectra demonstrated that the main structural changes of SPE-DOM from source to
379 mouth comprised a very significant oxidation of riverine SPE-DOM which referred to an
380 increasing abundance of both direct oxygenation products (OC**H**-units) and, even more
381 significant, carboxylation (R-C**H**$_n$-COOH units). The introduction of oxygen imposes remote
382 substituent effects on δ_H up to four bonds away. The superposition of much more numerous
383 different aliphatic chemical environments in the downstream reaches eventually produced
384 even more continual, broad NMR resonance envelopes at the expense of intense NMR
385 resonances originating from oxygen-depleted simple aliphatic branching motifs (Fig. 6C).
386 Broad NMR resonances poor in distinct features are characteristic of a highly processed
387 organic matter like those found in downstream SPE-DOM. The diversification of aliphatic
388 components along the river stretch corresponded well with the increased abundance of rather

389 aliphatic components with high H/C and low O/C ratios observed by FTICR MS. The slight
390 decrease of aromatic components indicated by NMR was in accordance with the decrease of
391 O-rich&DBE-richComp with low H/C and high O/C shown by FTICR MS.
392 Stoichiometry of DOM was shown to alter with changing land use (Gücker et al., 2016).
393 Holtemme River showed higher proportions of CHNO, CHOS and CHNOS compounds in
394 urbanized and agricultural areas compared to forest catchments (Fig. S2) in line with previous
395 results (Wagner et al., 2015). The observed increase in relative abundance of single CHOS
396 compounds and the group $CHOS_1$ O-poor downstream the WWTP (Fig. 5, Fig. S6)
397 corresponds to highly abundant CHOS compounds found in effluent organic matter by
398 Gonsior et al. (2011). The CHOS derived mass peaks with highest abundances in effluent
399 organic matter could be attributed to anthropogenic surfactants such as linear alkyl benzene
400 sulfonates, their co-products dialkyl tetralin sulfonates and their biodegraded metabolites such
401 as sulfophenyl carboxylic acids (Gonsior et al., 2011; Wang et al., 2018). As an example, the
402 component $C_{14}H_{20}O_5S$ is potentially a sulphenyl carboxylic acid and $C_{15}H_{20}O_5S$ a dialkyl
403 tetralin sulfonate intermediate (Gonsior et al., 2011). The molecular complexity can be
404 increased in effluent organic matter (Tseng et al., 2013). In contrast to the CHOS, the increase
405 of CHNO compounds (Fig. 4; Fig. S6) and the appearance of some CHNO compounds at site
406 6 (Fig. 4B) in Holtemme River can be explained by diffuse sources from agriculture. This was
407 confirmed the increase of CHN_1O and CHN_2O group between samples 5 and 6 (Fig. S6).
408 CHNO were also reported to originate from effluent organic matter (Mesfioui et al., 2012).
409 Several CHNO components increased after both WWTPs (e.g., $C_{14}H_{17}N_1O_8$; Fig. S6),
410 however, WWTPs seemed to be a minor source for CHNO compared to agriculture. As
411 sampling was performed under base flow conditions when the relative contribution of point
412 sources is expected to be high compared to diffuse sources, the importance of agricultural
413 CHNO import into the Holtemme River should be even higher at high discharge.
414

DOM diversity: natural decline versus increase by human activity and microbial oxygenation

The river continuum concept (RCC) (Vannote et al., 1980) proposed maximum molecular diversity of DOM in headwaters and a continual decrease of DOM molecular diversity downstream (Vannote et al., 1980). Fragmentation of ecosystems in mountainous headwater streams contributes to differences in DOM formation conditions on very small spatial scales, leading to increased molecular diversity (Mosher et al., 2015; Lynch et al., 2019) whereas larger water bodies such as higher order streams are subject to mixing, attenuation of gradients and equilibration of DOM formation conditions. This predicted pattern was confirmed by the results in the upper part of Holtemme River: DOM diversity based on FTICR mass spectrometry showed the highest number of compositions at site 1 (n = 2396) and remarkably declined toward site 4 (n = 969; Fig. 4c). NMR spectra demonstrated dominance of certain aliphatic branching motifs in the headwaters of Holtemme River (Fig. 6C). This does not necessarily imply the presence of a restricted count of diverse molecules but it means that the majority of these molecules share a certain set of oxygen-deficient aliphatic branching motifs (Hertkorn et al., 2015). NOM is commonly more oxygenated than biological metabolites and it carries significantly higher proportions of quaternary carbon atoms (Lam et al., 2007). Headwater DOM features mainly forest-derived organic matter which primarily consists of lignin- and tannin derived biogeochemical organic molecules of decent oxygenation and often lipid-derived common biomolecules which are highly aliphatic, with a low average degree of oxygenation. Therefore, initially produced DOM shows an intermediate degree of unsaturation and a relative depletion of heteroatoms.

However, the number of components increased again toward site 7 (n = 2543) and stayed nearly constant further downstream (Table S4). In-stream algal-derived primary production initially generates primarily aliphatic and rather oxygen-deficient lipid-derived metabolites (apart from fast cycling carbohydrates which are poorly retained by SPE and also do not ionize well in negative ESI). However, continual breakdown of larger size molecules and

aggregates is accompanied by progressive bacterial oxidation of riverine DOC and POC. Here, oxygen is introduced on a massive scale to produce carboxyl-rich alicyclic molecules (CRAM; Hertkorn et al., 2006; Lam et al., 2007), materials derived from linear terpenoids (MDLT; Lam et al., 2007; Arakawa et al., 2017) and many other oxidation products with an overall higher compositional and structural diversity than found in the starting materials. In Holtemme River, human activities like agriculture and WWTP probably have contributed to introduction of CHNO, CHOS and CHNOS compounds into riverine DOM (Fig 4B; Table S4) some of it also through groundwater input (Graham et al., 2018).

In the most downsteam reaches of Holtemme, it becomes progressively more difficult to determine changes in the composition (by FTICR-MS) and structure (by NMR) of riverine DOM. Evolved DOM is subject to a myriad of biochemical transformations which nevertheless are dominated by a very few nominal transformations (Moritz et al., 2017) such as e.g. hydroxylation (±O), methylation (±CH_2), (de)hydration (±H_2O), glycosylation (±$C_6H_{12}O_6$), (de)acetylation (±C_2H_2O) and carboxylation (±CO_2) which are imposed on already pre-existing DOM molecules. With an appreciable coverage of the compositional space already in place (Hertkorn et al., 2008), the vast majority of these reactions will project on compositions already present in the mixture (Fig. S13).

Compound-specific links to bacterial activity

Low values of planktonic BP were observed in the headwater sections at high DOC concentrations since the DOM was dominated by O-rich&DBE-richComp. The quality of the DOM was obviously more important than its concentration which had also been reported by Shi et al. (2016). The planktonic BP was enhanced with rising nitrate concentration (site 3), and it further increased downstream of the two WWTPs (from site 4 to 5 and from site 7 to 8). Planktonic abundance and BP were particularly correlated to oxygen-poor CHOS components released by the WWTPs (Fig. S14c). In Maine (US), decreased proportions of humic-like

allochthonous DOM and increased abundance of bioavailable autochthonous DOC amounts in urbanized streams doubled the DOC decay rate and increased the activity of carbon-acquiring enzymes (Parr et al., 2015). In headwaters, microbial bioavailability of DOM was greater in urbanized streams with decreasing proportions of humic-like DOM and increasing proportions of protein-like DOM (Hosen et al., 2014). In contrast, the long-term bacterial growth did not mirror the longitudinal dynamics of BP in our study, it was high at WWTP A at site 5 (but not at WWTP B) followed by a subsequent decrease and downstream a weir (site 10) where the stagnant water might have changed bacterial community composition. Usually, effluents of WWTPs increase the number of live bacteria, extracellular enzyme activity (Perujo et al., 2016), leucine aminopeptidase activity, and respiration (Aristi et al., 2015) compared to the upstream sites.

Planktonic BP increased with decreasing HIX and increasing β/α as already observed for the whole Bode catchment (Kamjunke et al., 2015). Lower HIX and higher β/α values had suggested an enhanced BP in agricultural streams previously (Williams et al., 2010). This could be corroborated by many negatively correlated FTICR MS components with planktonic BP. Of those many were O-rich&DBE-richComp which are shown to positively correlate with the HIX (Fig. S6) as confirmed by literature (Lavonen et al., 2015; Herzsprung et al., 2017). The positive correlation of planktonic BP to β/α can be explained by many positively correlated components with more aliphatic character (H/C > 1 for most of them). Negative correlation may either mean that the component was more consumed if BP was high or that BP was inhibited. Simple correlations alone would not enable distinction of these two types of DOM processing. Biofilm BP showed less variability compared to planktonic BP and was not related to bulk DOM characteristics such as HIX and β/α as described before (Kamjunke et al., 2015). With the recognition of FTICR MS-derived molecular compositions, only few correlations were found for biofilms which was true also for long-term bacterial growth. The mainly positive slopes of NMR intensities over the river stretch in the range δ_H ~1-5 ppm

493 (Fig. 6C) coincided with mainly positive correlations between the respective NMR section
494 integrals and planktonic and biofilm BP (Fig. 9). This indicates that the increase of NMR
495 components was positively related to BP. The increase of NMR slopes in downstream
496 direction between δ_H ~7-8 ppm positively correlated with planktonic and biofilm BP
497 indicating a microbial production of aromatic carboxylic acids.
498

499 **5. Conclusion**

500 While the massive dislocation of oxygen observed in DOM along the river course of river
501 Holtemme probably occurred from natural causes operating in pristine rivers, sizable
502 proportions of CHOS, CHNO and CHNOS compounds were introduced in downstream
503 reaches by anthropogenic activities. The decrease of DOM diversity in the upper part of
504 Holtemme (hypothesis 1) was predicted by the river continuum concept (RCC) and reflected
505 the transition from fragmented ecosystems in Holtemme headwaters with a high diversity of
506 DOM formation conditions to a larger water body with attenuated gradients, extensive mixing
507 and more uniform conditions. The influence of the WWTPs was apparent by an increase of
508 the freshness index, decreasing oxidation state of carbon, and an increase of several CHOS
509 components. Mass spectrometry and NMR spectroscopy of DOM along the Holtemme river
510 course revealed relationships between DOM composition and bacterial activity which were
511 not available from fluorescence indices (hypothesis 2). Further research should clarify the
512 relative contributions of pristine in-river processing of DOM and competing anthropogenic
513 influences on the evolution of CHOS, CHNO and CHNOS compounds.
514

515 **Acknowledgements**

We thank Ute Link for measuring bacterial production, Ina Siebert for DOC determination, Sigrid Kaschuba and Nina Weber for AOC measurements, Ines Locker for SPE, and two anonymous reviewers for their helpful comments.

This research did not receive any specific grant from funding agencies in the public, commercial, or not-for-profit sectors.

521 **References**

522 Arakawa, N., Aluwihare, L. I., Simpson, A. J., Soong, R., Stephens, B. M., Lane-Doplen D.,
523 2017. Carotenoids are the likely precursor of a significant fraction of marine dissolved
524 organic matter. Sci. Adv. 3, e1602976.
525 Aristi, I., von Schiller, D., Arroita, M., Barcelo, D., Ponsati, L., Garcia-Galan, M. J., Sabater,
526 S., Elosegi, A., Acuna, V., 2015. Mixed effects of effluents from a wastewater treatment
527 plant on river ecosystem metabolism: subsidy or stress? Freshwater Biol. 60, 1398-1410.
528 Arnold, W.A., Longnecker, C., Kroeger, K.D., Kujawinski, E.B., 2014. Molecular signature
529 of organic nitrogen in septic impacted groundwater Environ. Sci. – Processes & Impacts
530 16, 2400-2407.
531 Aufdenkampe, A.K., Mayorga, E., Raymond, P.A., Melack, J.M., Doney, S.C., Alin, S.R.,
532 Aalto, R.E., Yoo, K., 2011. Riverine coupling of biogeochemical cycles between land,
533 oceans, and atmosphere. Front. Ecol. Environ. 9, 53-60.
534 Battin, T.J., Kaplan, L.A., Newbold, J.D., Hansen, C.M., 2003. Contributions of microbial
535 biofilms to ecosystem processes in stream mesocosms. Nature 426: 439-442.
536 Battin, T.J., Kaplan, L.A., Findlay, S., Hopkinson, C.S., Marti, E., Packman, A.I., Newbold,
537 J.D., Sabater, F., 2008. Biophysical controls on organic carbon fluxes in fluvial networks.
538 Nature Geosci. 1, 95-100.
539 Bodmer, P., Heinz, M., Pusch, M., Singer, G., Premke, K., 2016. Carbon dynamics and their
540 link to dissolved organic matter quality across contrasting stream ecosystems. Sci. Total
541 Environ. 553, 574-586.
542 Cole, J.J., Prairie, Y.T., Caraco, N.F., McDowell, W.H., Tranvik, L., Striegl, R.G., Duarte,
543 C.M., Kortelainen, P., Downing, J.A., Middelburg, J.J., Melack, J.M., 2007. Plumbing the
544 global carbon cycle: integrating inland waters into the terrestrial carbon budget.
545 Ecosystems 10, 171-184.

546 Cory, R.M., Kaplan, L.A., 2012. Biological lability of streamwater fluorescent dissolved
547 organic matter. Limnol. Oceanogr. 57, 1347-1360.
548 Dadi, T., Harir, M., Hertkorn, N., Koschorreck, M., Schmitt-Kopplin, P., Herzsprung, P.,
549 2017. Redox conditions affect dissolved organic carbon quality in stratified freshwaters.
550 Environ. Sci. Technol. 51, 13705 – 13713.
551 Dittmar, T., Koch, B., Hertkorn, N., Kattner, G., 2008. A simple and efficient method for the
552 solid-phase extraction of dissolved organic matter (SPE-DOM) from seawater. Limnol.
553 Oceanogr.: Methods 6, 230-235.
554 Ejarque, E., Freixa, A., Vazquez, E., Guarch, A., Amalfitano, S., Fazi, S., Romani, A.M.,
555 Butturini, A., 2017. Quality and reactivity of dissolved organic matter in a Mediterranean
556 river across hydrological and spatial gradients. Sci. Total Environ. 599-600, 1802-1812.
557 Fellman, J.B., Hood, E., Spencer, R.G.M., 2010. Fluorescence spectroscopy opens new
558 windows into dissolved organic matter dynamics in freshwater ecosystems: A review.
559 Limnol. Oceangr. 55, 2452-2462.
560 Gonsior, M., Zwartjes, M., Cooper, W.J., Song, W., Ishida, K.P., Tseng, L.Y., Jeung, M.K.,
561 Rosso, D., Hertkorn, N., Schmitt-Kopplin, P., 2011. Molecular characterization of effluent
562 organic matter identified by ultrahigh resolution mass spectrometry. Wat. Res. 45, 2943-
563 2953.
564 Graeber, D., Boechat, I.G., Encina-Montoya, F., Esse, C., Gelbrecht, J., Goyenola, G.,
565 Gücker, B., Heinz, M., Kronvang, B., Meerhoff, M., Nimptsch, J., Pusch, M., Silva,
566 R.C.S., von Schiller, D., Zwirnmann, E., 2015. Global effects of agriculture on fluvial
567 dissolved organic matter. Sci. Rep. 5, 16328.
568 Graham, E. B., Crump, A.R., Kennedy, D.W., Arntzen, E., Fansler, S., Purvine, S. O., Nicora,
569 C. D., Nelson, W., Tfaily, M. M., Stegen, J. C., 2018. Multi´omics comparison reveals
570 metabolome biochemistry, not microbiome composition or gene expression, corresponds to
571 elevated biogeochemical function in the hyporheic zone. Sci. Total Environ. 642, 742-753.

572 Gücker, B., Silva, R. C. S., Graeber, D., Monteiro, J. A. F., Boechat, I. G., 2016. Urbanization
573 and agriculture increase exports and differentially alter elemental stoichiometry of
574 dissolved organic matter (DOM) from tropical catchments. Sci. Total Environ. 550, 785-
575 792.
576 Hale, R.L., Godsey, S.E., 2019. Dynamic stream intermittence explains emergent dissolved
577 organic carbon chemostasis in headwaters. Hydrol. Processes, doi: 10.1002/hyp.13455
578 Hertkorn, N., Benner, R., Frommberger, M., Schmitt-Kopplin, P., Witt, M., Kaiser, K.,
579 Kettrup, A., Hedges, J. I., 2006. Characterization of a major refractory component of
580 marine dissolved organic matter. Geochim. Cosmochim. Acta 70, 2990-3010.
581 Hertkorn, N., Ruecker, C., Meringer, M., Gugisch, M. Frommberger, M., Perdue, E.M. Witt,
582 M., Schmitt-Kopplin, P., 2007. High-precision frequency measurements: indispensable
583 tools at the core of the molecular-level analysis of complex systems. Anal. Bioanal. Chem.
584 389, 1311–1327.
585 Hertkorn, N., Frommberger, M., Witt, M., Koch, B.P., Schmitt-Kopplin, P., Perdue, E.M.,
586 2008. Natural organic matter and the event horizon of mass spectrometry. Anal. Chem. 80,
587 8908-8919.
588 Hertkorn, N., Harir, M., Schmitt-Kopplin, P., 2015. Non target analysis of Murchison soluble
589 organic matter by high-field NMR spectroscopy and FTICR mass spectrometry. Magn.
590 Reson. Chem. 53, 754–768.
591 Hertkorn, N., Harir, M., Cawley, K. M., Schmitt-Kopplin, P., Jaffe, R., 2016. Molecular
592 characterization of dissolved organic matter from subtropical wetlands: a comparative
593 study through the analysis of optical properties, NMR and FTICR/MS. Biogeosciences 13,
594 1-21.
595 Herzsprung, P., von Tümpling, W., Hertkorn, N., Harir, M., Büttner, O., Bravidor, J., Friese,
596 K., Schmitt-Kopplin, P., 2012. Variations of DOM quality in inflows of a drinking water

reservoir: Linking of van Krevelen diagrams with EEMF spectra by rank correlation. Environ. Sci. Technol. 46, 5511 – 5518.

Herzsprung, P., Osterloh, K., von Tümpling, W., Harir, M., Hertkorn, N., Schmitt-Kopplin, P., Meissner, R., Bernsdorf, S., Friese, K., 2017. Differences in DOM of rewetted and natural peatlands – results from high-field FT-ICR-MS and bulk optical parameters. Sci. Tot. Environ. 586, 770-781.

Hosen, J.D., McDonough, O.T., Febria, C.M., Palmer, M.A., 2014. Dissolved organic matter quality and bioavailability changes across an urbanization gradient in headwater streams. Environ. Sci. Technol. 48, 7817-7824.

Jaffe, R., Yamashita, Y, Maie, N., Cooper, W.T., Dittmar, T., Dodds, W.K., Jones, J.B., Myoshi, T., Ortiz-Zayas, J.R., Podgorski, D.C., Watanabe, A., 2012. Dissolved organic matter in headwater streams: Compositional variability across climatic regions of North America. Geochim. Cosmochim. Acta 94, 95-108.

Kamjunke, N., Büttner, O., Jäger, C.G., Marcus, H., von Tümpling, W., Halbedel, S., Norf, H., Brauns, M., Baborowski, M., Wild, R., Borchardt, D., Weitere, M., 2013. Biogeochemical patterns in a river network along a land use gradient. Environ. Monit. Assess. 185, 9221-9236.

Kamjunke, N., Herzsprung, P., Neu, T. R., 2015. Quality of dissolved organic matter affects planktonic but not biofilm bacterial production in streams. Sci. Total Environ. 506-507, 353-360.

Kamjunke, N.; von Tümpling, W.; Hertkorn, N.; Harir, M.; Schmitt-Kopplin, P.; Norf, H.; Weitere, M.; Herzsprung, P., 2017. A new approach for evaluating transformations of dissolved organic matter (DOM) via high-resolution mass spectrometry and relating it to bacterial activity. Water Res., 123, 513-523.

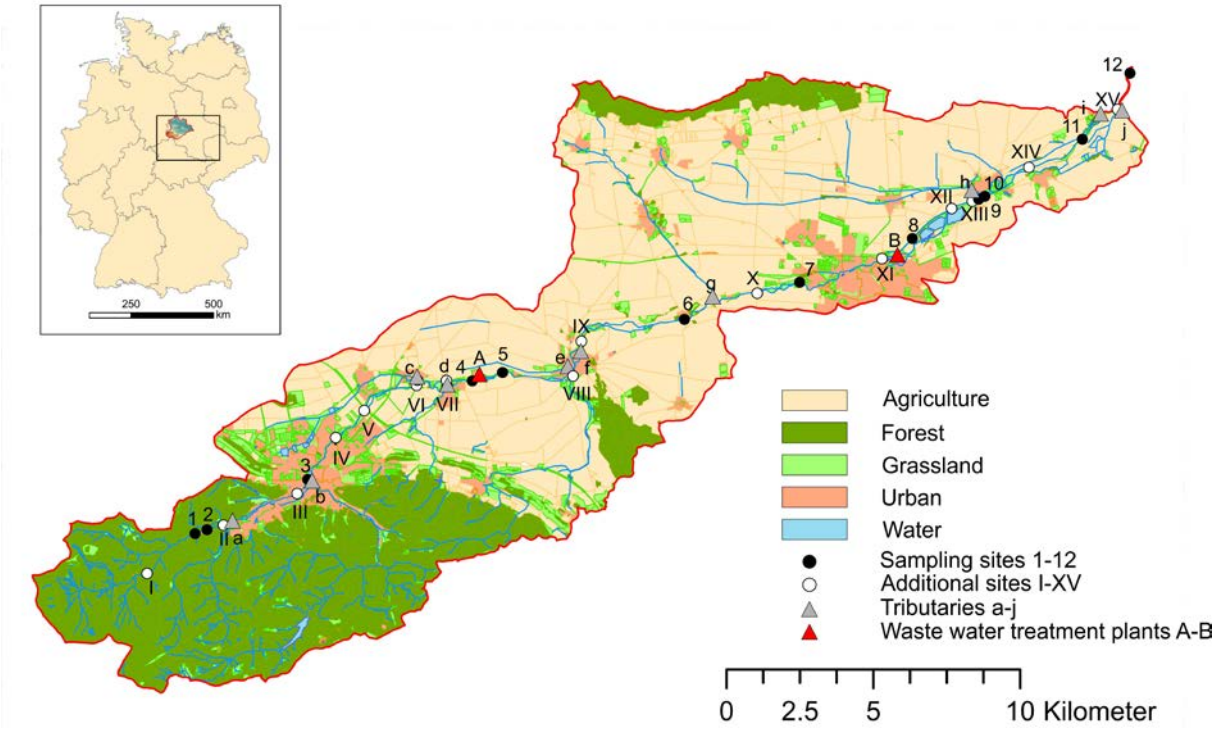
621 Kim, S., Kaplan, L.A., Hatcher, P.G. 2006. Biodegradable dissolved organic matter in a
622 temperate and a tropical stream determined from ultra-high resolution mass spectrometry.
623 Limnol. Oceanogr. 51: 1054-1063
624 Lam, B., Baer, A., Alaee, M., Lefebvre, B., Moser, A., Williams, A., Simpson, A. J., 2007.
625 Major structural components in freshwater dissolved organic matter. Environ. Sci.
626 Technol. 41, 2840-2847.
627 Lavonen, E.E., Kothawala, D.N., Tranvik, L.J., Gonsior, M., Schmitt-Kopplin, P., Köhler,
628 S.J., 2015. Tracking changes in the optical properties and molecular composition of
629 dissolved organic matter during drinking water production. Water Res. 85, 286–294.
630 Lynch, L.M., Sutfin N.A., Fegel, S.T., Boot, C.M., Covino, T.P., Wallenstein, M.D., 2019.
631 River channel connectivity shifts metabolite composition and dissolved organic matter
632 chemistry. Nat. Comm. 10, 459.
633 Meckenstock, R.U., von Netzer, F., Stumpp, C., Lueders, T., Himmelberg, A.M, Hertkorn, N.,
634 Schmitt-Kopplin, P., Harir, M., Hosein, R., Haque, S., Schulze-Makuch, D., 2014. Water
635 droplets in oil are microhabitats for microbial life. Science 345, 673-676.
636 Mesfioui, R., Love, N.G., Bronk, D.A., Mulholland, M.R., Hatcher, P.G., 2012. Reactivity
637 and chemical characterization of effluent organic nitrogen from wastewater treatment
638 plants determined by Fourier transform ion cyclotron resonance mass spectrometry. Wat.
639 Res. 46, 622-634.
640 Moritz, F., Kaling, M., Schnitzler, J. P., Schmitt-Kopplin, P., 2017. Characterization of poplar
641 metabolites via mass difference enrichment analysis. Plant Cell Environ., 40, 1057-1073.
642 Mosher, J.J., Kaplan, L.A., Podgorski, D.C., McKenna, A.M., Marshall, A.G. 2015.
643 Longitudinal shifts in dissolved organic matter chemogeography and chemodiversity
644 within headwater streams: a river continuum reprise. Biogeochemistry 124, 371-385

645 Osterholz, H., Kirchman, D.L., Niggemann, J., Dittmar, T., 2016. Environmental drivers of
646 dissolved organic matter molecular composition in the Delaware Estuary. Front. Earth Sci.
647 4, 95.
648 Parr, T.B., Cronan, C.S., Ohno, T., Findlay, S.E.G., Smith, S.M.C., Simon, K.S. 2015.
649 Urbanization changes the composition and bioavailability of dissolved organic matter in
650 headwater streams. Limnol.Oceanogr. 60: 885-900.
651 Perujo, N., Freixa, A., Vivas, Z., Gallegos, A. M., Butturini, A., Romani, A. 2016. Fluvial
652 biofilms from upper and lower river reaches respond differently to wastewater plant inputs.
653 Hydrobiologia 765: 169-183.
654 Raeke, J., Lechtenfeld, O.J., Wagner, M., Herzsprung, P., Reemtsma, T., 2016. Selectivity of
655 solid phase extraction of freshwater dissolved organic matter and its effect on ultrahigh
656 resolution mass spectra. Environ. Sci. – Processes & Impacts 18, 918 – 927.
657 Riedel, T., Dittmar, T., 2014. A method detection limit for the analysis of natural organic
658 matter via Fourier transform ion cyclotron resonance mass spectrometry. Anal. Chem. 86,
659 8376-8382.
660 Riedel, T., Zark, M., Vähätalo, A. V., Niggemann, J., Spencer, R. G. M., Hernes, P. J.,
661 Dittmar, T., 2016. Molecular signatures of biogeochemical transformationsin dissolved
662 organic matter from ten world rivers. Front. Earth Sci. 4, B5.
663 Rossel, P.E., Stubbins, A., Rebling, T., Koschinsky, A., Hawkes, J.A., Dittmar, T., 2017.
664 Thermally altered marine dissolved organic matter in hydrothermal fluids. Org. Geochem.
665 110, 73-86.
666 Sachs, L., 1974. Angewandte Statistik. Springer, Berlin, Heidelberg, New York.
667 Seifert, A.-G., Roth, V.-N., Dittmar, T., Gleixner, G., Breuer, L., Houska, T., Marxsen, J.,
668 2016. Comparing molecular composition of dissolved organic matter in soil and stream
669 water: Influence of land use and chemical characteristics. Sci. Total Environ. 571: 142-
670 152.

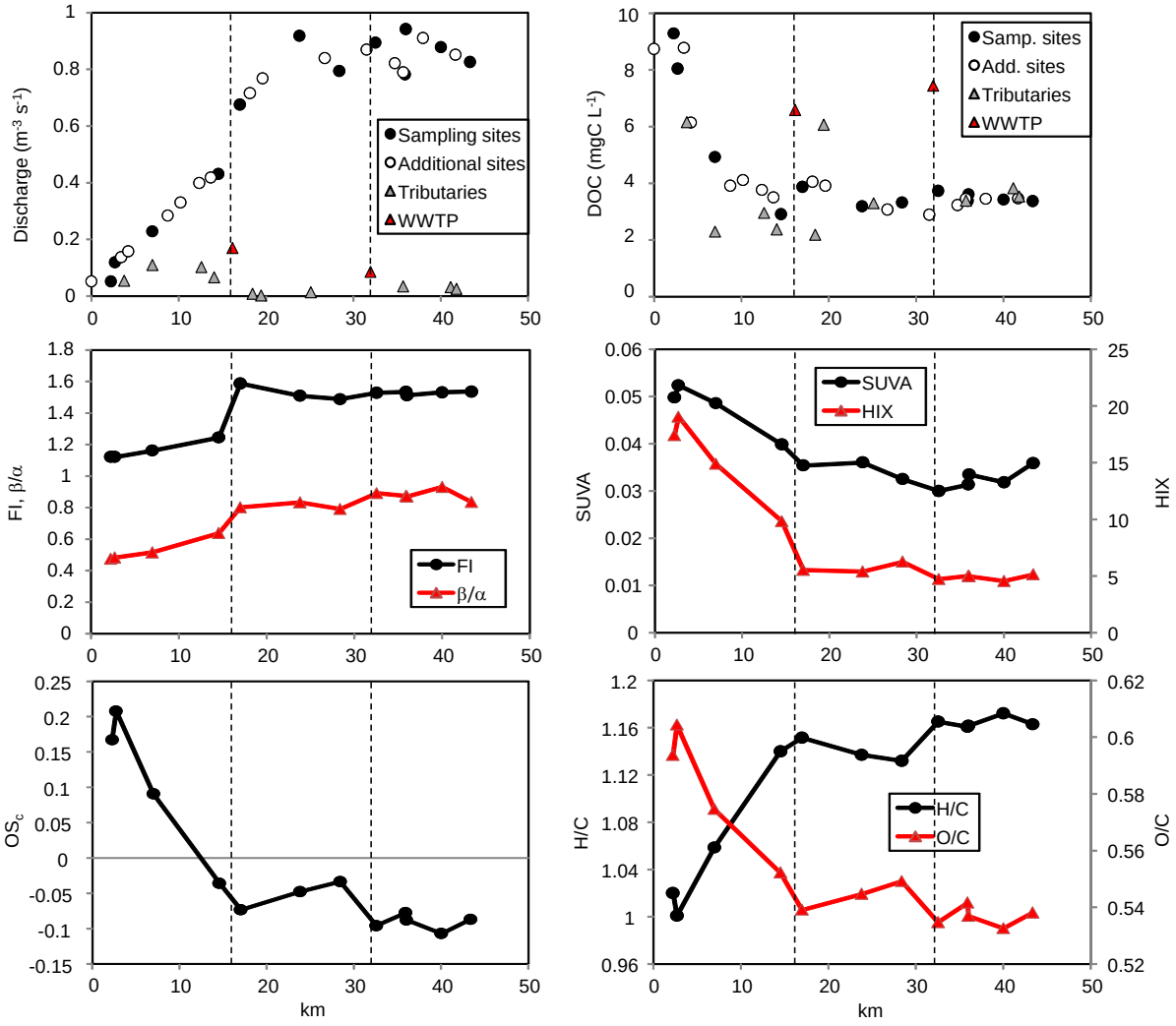
671 Shi, J., Cui, H., Jia, L., Qiu, L., Zhao, Y., Wei, Z., Wu, J., Wen, X., 2016. Bioavailability of
672 riverine dissolved organic carbon and nitrogen in the Heilongjiang watershed of
673 northeastern China. Environ. Monit. Assess. 188, 113.
674 Simon, M., Azam, F., 1989. Protein content and protein synthesis rates of planktonic bacteria.
675 Mar. Ecol. Prog. Ser. 51, 201-213.
676 Sleighter, R.L., Cory, R.M., Kaplan, L.A., Abdulla, H.A.N., Hatcher, P.G., 2014. A coupled
677 geochemical and biogeochemical approach to characterize the bioreactivity of dissolved
678 organic matter from a headwater stream. J. Geophys. Res. Biogeosci., 119, 1520–1537,
679 doi:10.1002/2013JG002600.
680 Stubbins, A., Spencer, R.G.M., Chen, H., Hatcher, P.G., Mopper, K., Hernes, P.J., Mwamba,
681 V.L., Mangangu, A.M., Wabakanghanzi, J.N., Six, J., 2010. Illuminated darkness:
682 molecular signatures of Congo River dissolved organic matter and its photochemical
683 alteration as revealed by ultrahigh precision mass spectrometry. Limnol. Oceanogr. 55,
684 1467-1477.
685 Tseng, L.Y., Gonsior, M., Schmitt-Kopplin, P., Cooper, W.J., Pitt, P., Rosso, D., 2013.
686 Molecular characteristics and differences of effluent organic matter from parallel activated
687 sludge and integrated fixed-film activated sludge (IFAS) processes. Environ. Sci. Technol.
688 47, 10277-10284.
689 Vannote, R.L., Minshall, G.W., Cummins, K.W., Sedell, J.R., Cushing, C.E.1980. River
690 continuum concept. Can. J. Fish. Aquat. Sci. 37, 130-137.
691 Wagner, S., Riedel, T., Niggemann, J., Vähätalo, A.V., Dittmar, T., Jaffe, R. 2015. Linking
692 molecular signature of heteroatomic dissolved organic matter to watershed characteristics
693 in world rivers. Environ. Sci. Technol. 49: 13798-13806.
694 Wang, X., Wang, J., Li, K., Zhang, H., Yang, M., 2018. Molecular characterization of effluent
695 organic matter in secondary effluent and reclaimed water: Comparison to natural organic
696 matter in source water. J. Environ. Sci. 63, 140-146.

697 Williams, C.J., Yamashita, Y., Wilson, H.-F., Jaffe, R., Xenopoulos, M.A., 2010. Unraveling
698 the role of land use and microbial activity in shaping dissolved organic matter
699 characteristics in stream ecosystems. Limnol. Oceanogr. 55,1159-1171.
700 Wollschläger, U., Attinger, S., Borchardt, D., Brauns, M., Cuntz, M., Dietrich, P. et al., 2017.
701 The Bode hydrological observatory: a platform for integrated, interdisciplinary hydro-
702 ecological research within the TERENO Harz/Central German Lowland Observatory.
703 Environ. Earth Sci. 76, 29
704 Zsolnay, A., 2003. Dissolved organic matter: artefacts, definitions, and functions. Geoderma
705 113,187-209.
706

Fig. 1: Map of the investigated river stretch showing 12 main sampling sites, additional sampling sites, tributaries, waste water treatment plants, land use, and the position within Germany (insert).

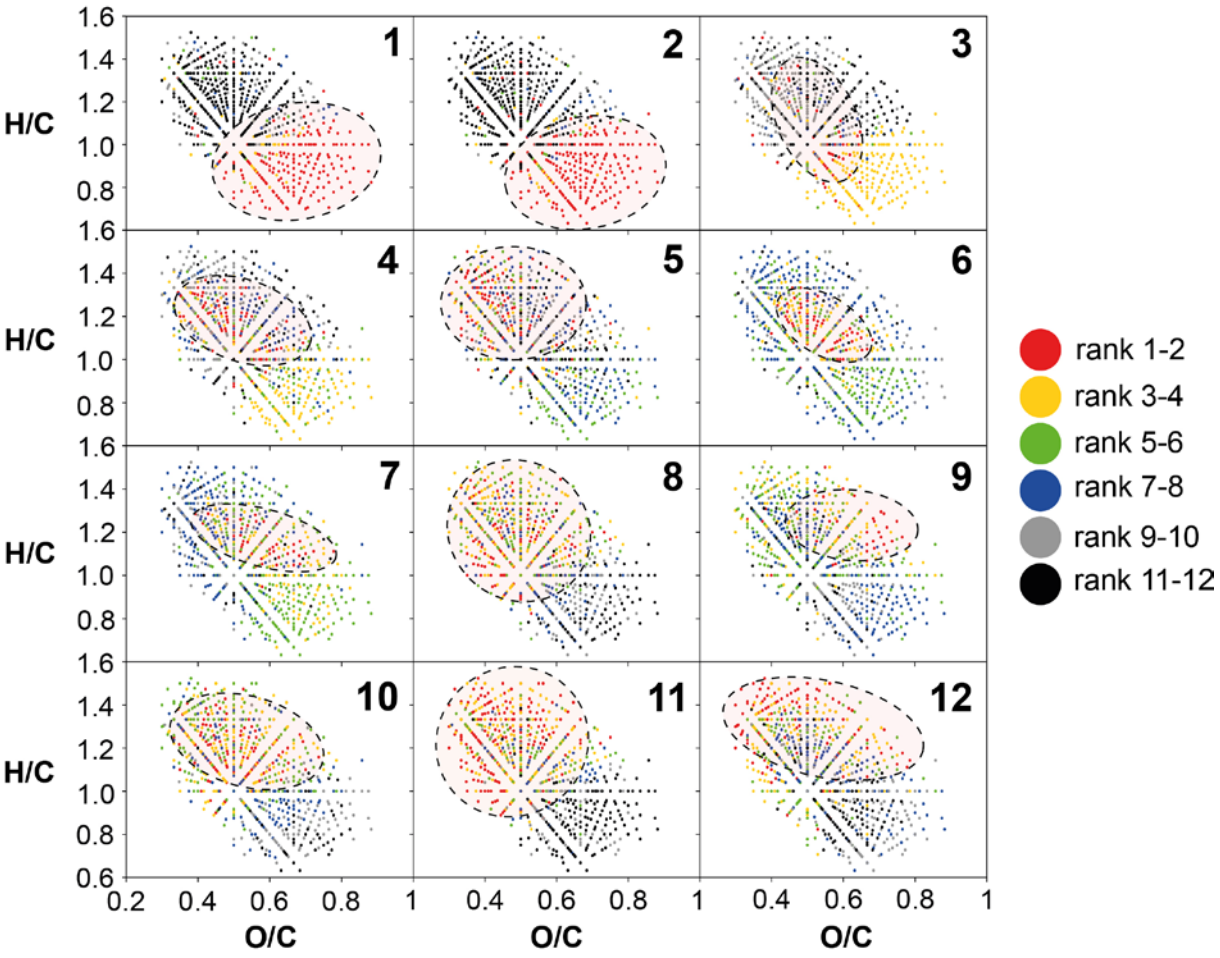


711 Fig. 2: Longitudinal dynamics of discharge and DOM properties : DOC concentration, FI:
712 fluorescence index, β/α: freshness index, HIX: humification index, SUVA: specific UV
713 absorption, OS_c: oxidation state of carbon, O/C and H/C ratios. Dashed lines mark the
714 WWTPs.



715

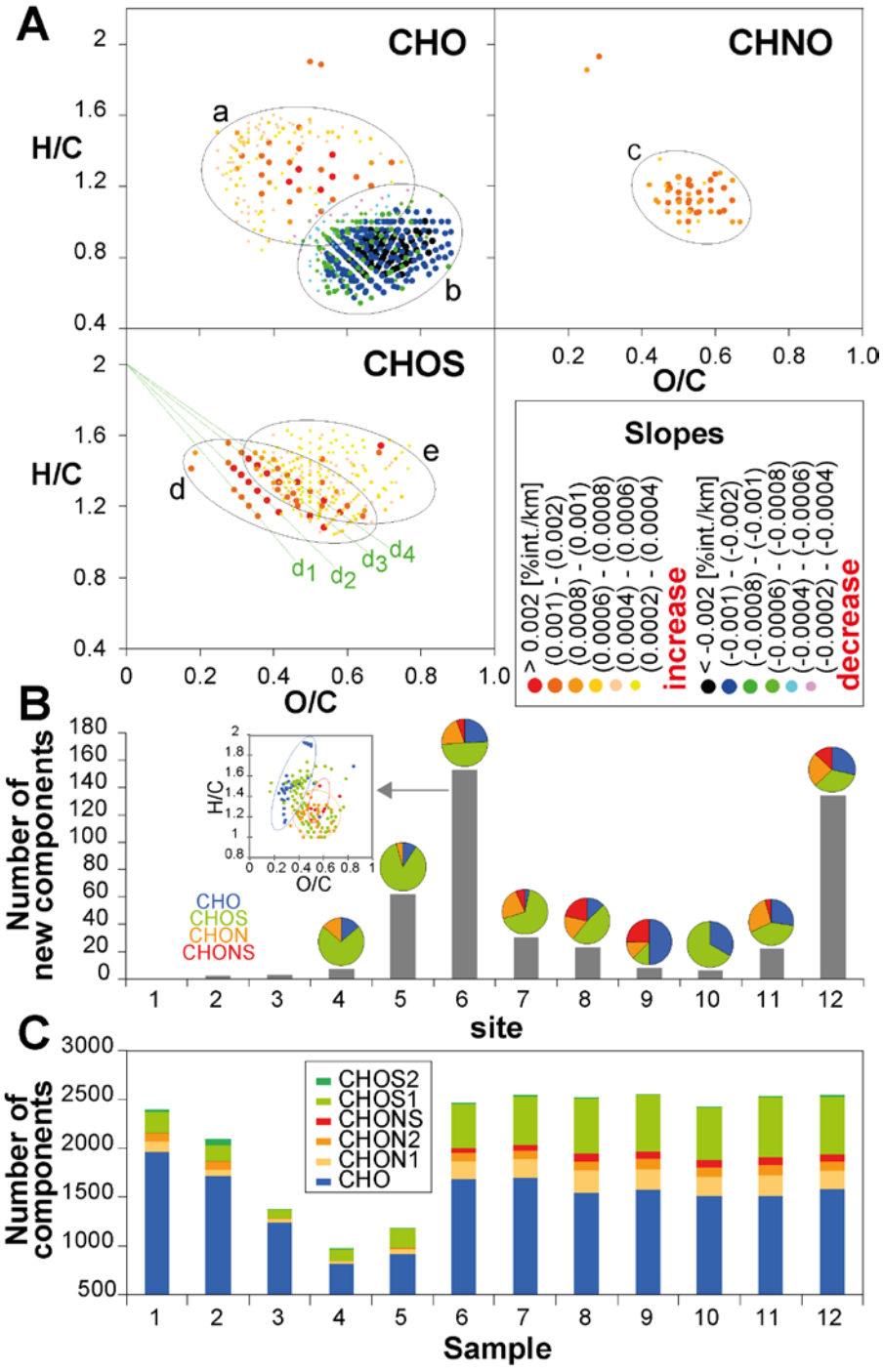
716 Fig. 3: Inter sample-ranks of FTICR MS components comparing all 12 samples, with highest
717 ranks 1-2 indicated by ellipsoids for clarity.



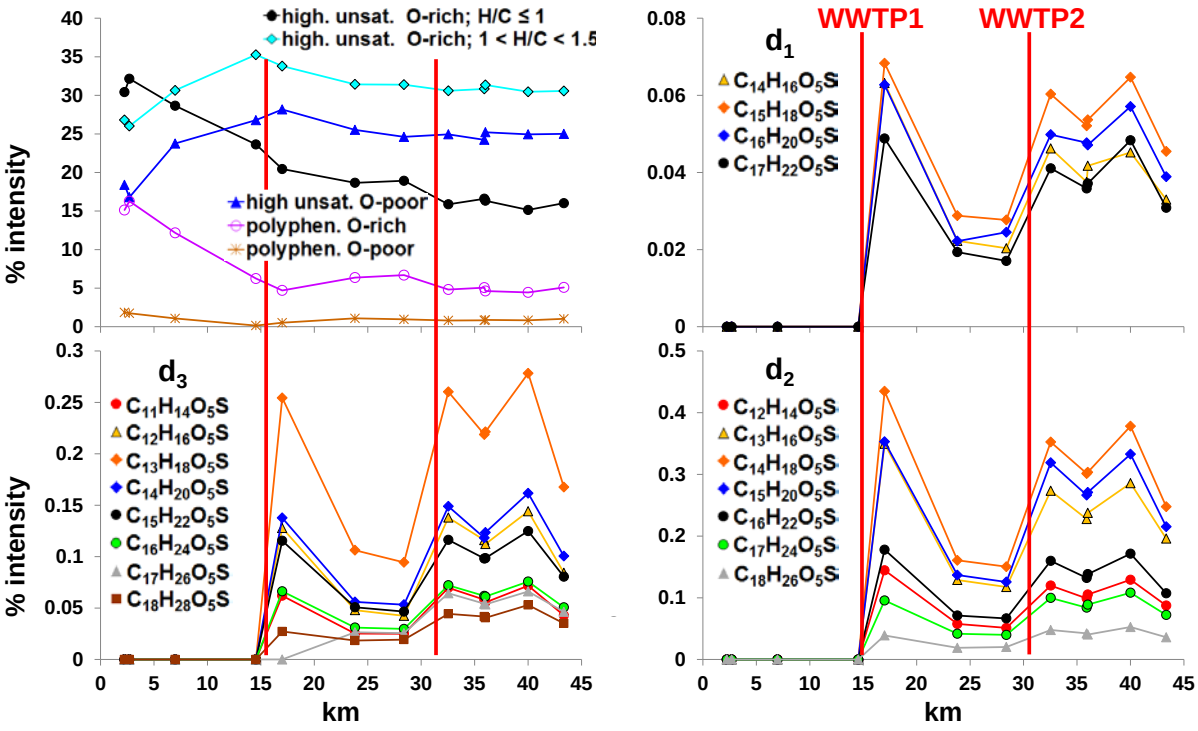
718

719

Fig 4: FTICR MS-derived evolution of DOM along Holtemme river course. Panel A: van Krevelen diagrams derived from the slopes of relative mass peak intensities along the river stretch sorted according to CHO, CHNO and CHOS molecular series. For attribution of section cf. main text and for attribution of CHOS-based molecular series $d_{1\text{-}4}$ cf. Table S6. Panel B: counts of compositions and relative proportions of CHO, CHOS, CHNO and CHNOS molecular series present in the given sampling point and in *all* consecutive sampling points downstream (cf. text), providing a relevant measure of relative persistence and emphasis of differences in DOM compositions between adjacent sampling points. At site 6, the suite of CHNO compounds showed considerable oxygenation and unsaturation as depicted in the van-Krevelen diagram (insert). c) number of FTICR MS components at 12 sampling sites.

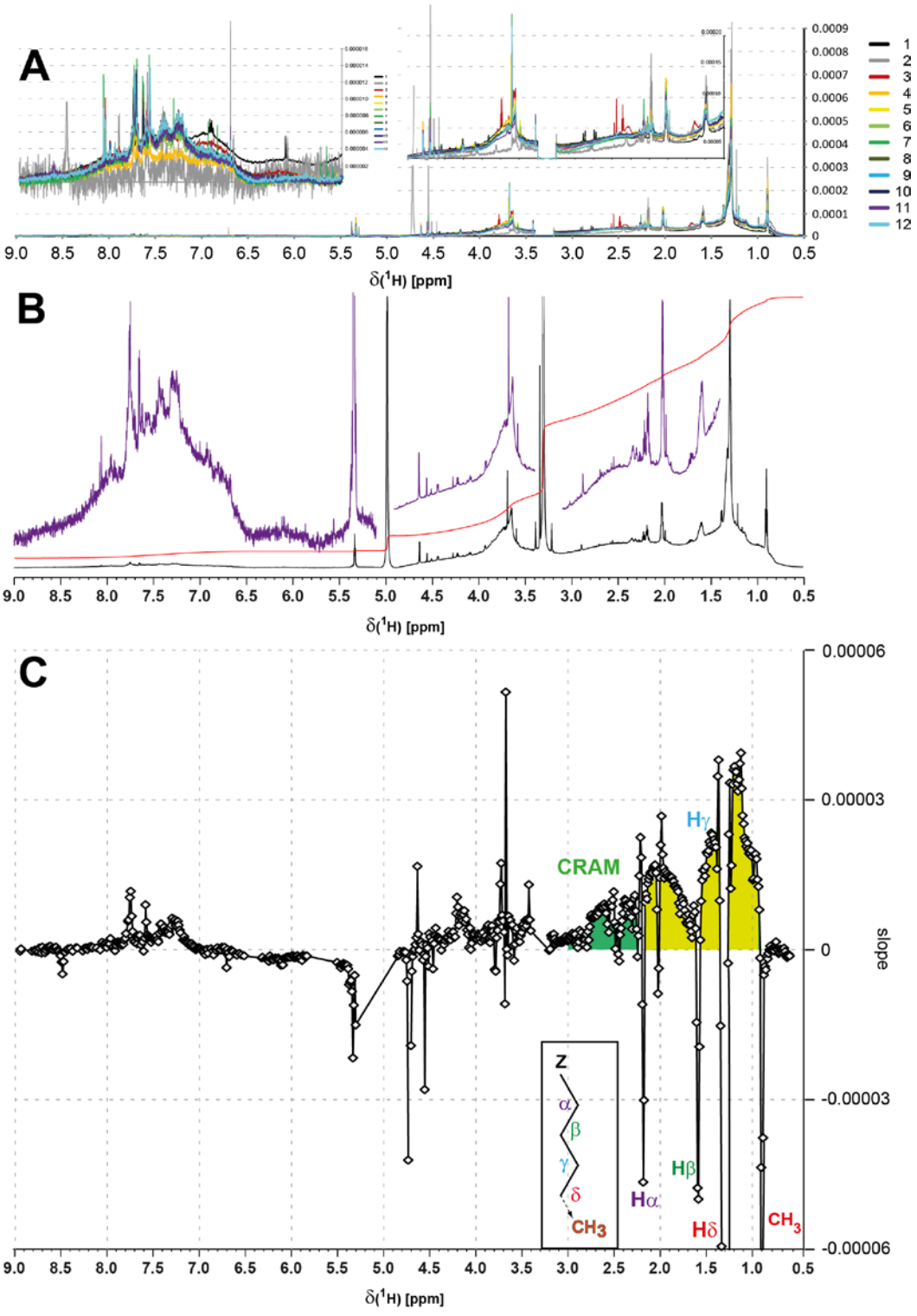


732 Fig. 5: Longitudinal dynamics of several groups of FTICR MS components (top left) and of
733 CHOS components of lines d_1-d_3 (see Fig. 4). Red lines mark the WWTPs.

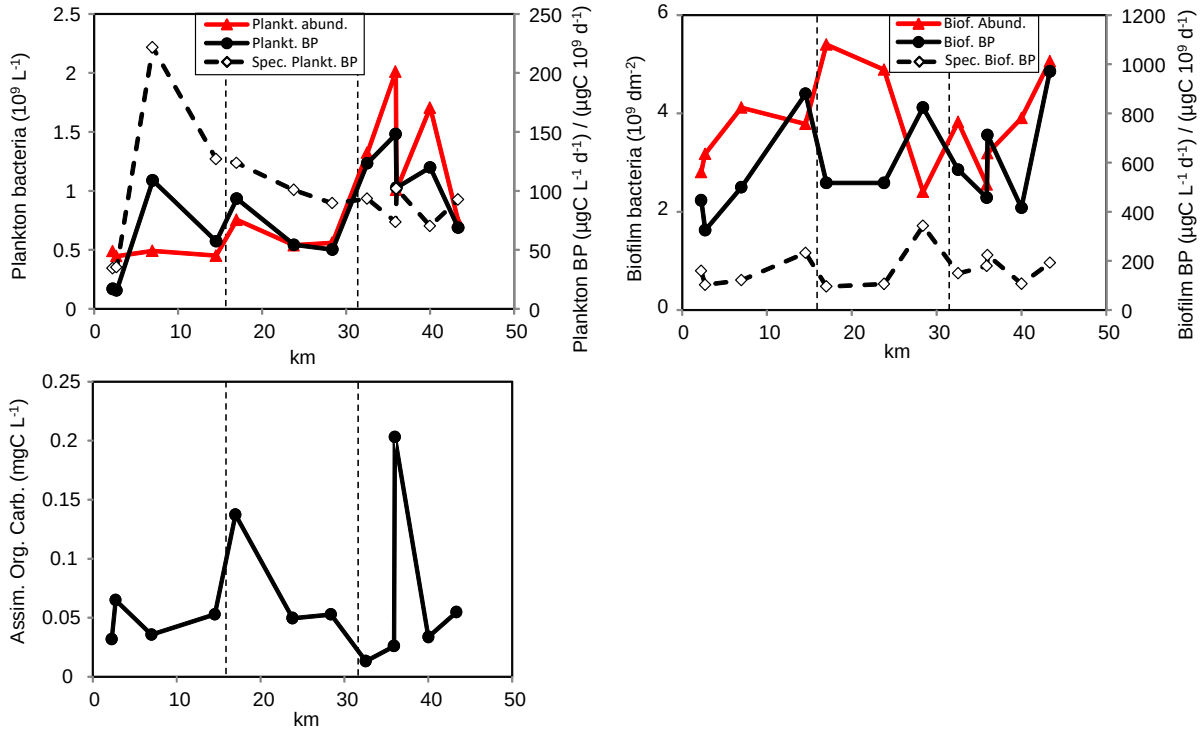


734

Fig. 6: ^{1}H NMR spectra (800 MHz, CD_3OD) of SPE-DOM (PPL) of sites 1-12. Panel A: overlay of area-normalized ^{1}H NMR spectra of SPE-DOM; panel B: example ^{1}H NMR spectrum of SPE-DOM of site 5. Panel C: slopes of NMR section integrals with 0.01 ppm resolution as computed from area-normalized ^{1}H NMR spectra along the river course from source to outflow; positive/negative slopes indicate growth/decrease in relative abundance along the river course (cf. text).

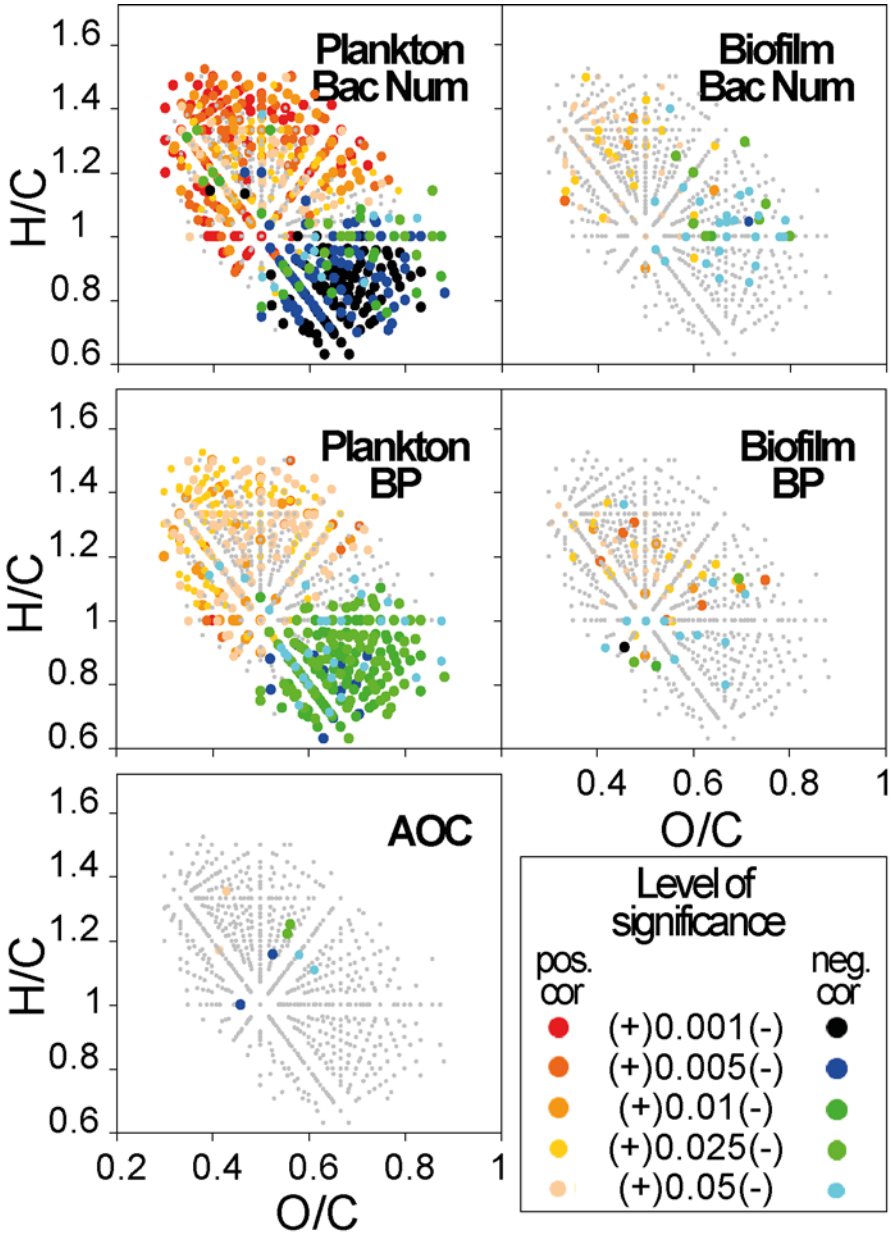


742 Fig. 7: Longitudinal dynamics of bacterial abundance, bacterial production (BP), cell-specific
743 BP of plankton and biofilm bacteria, and assimilable organic carbon. Dashed lines mark the
744 WWTPs.



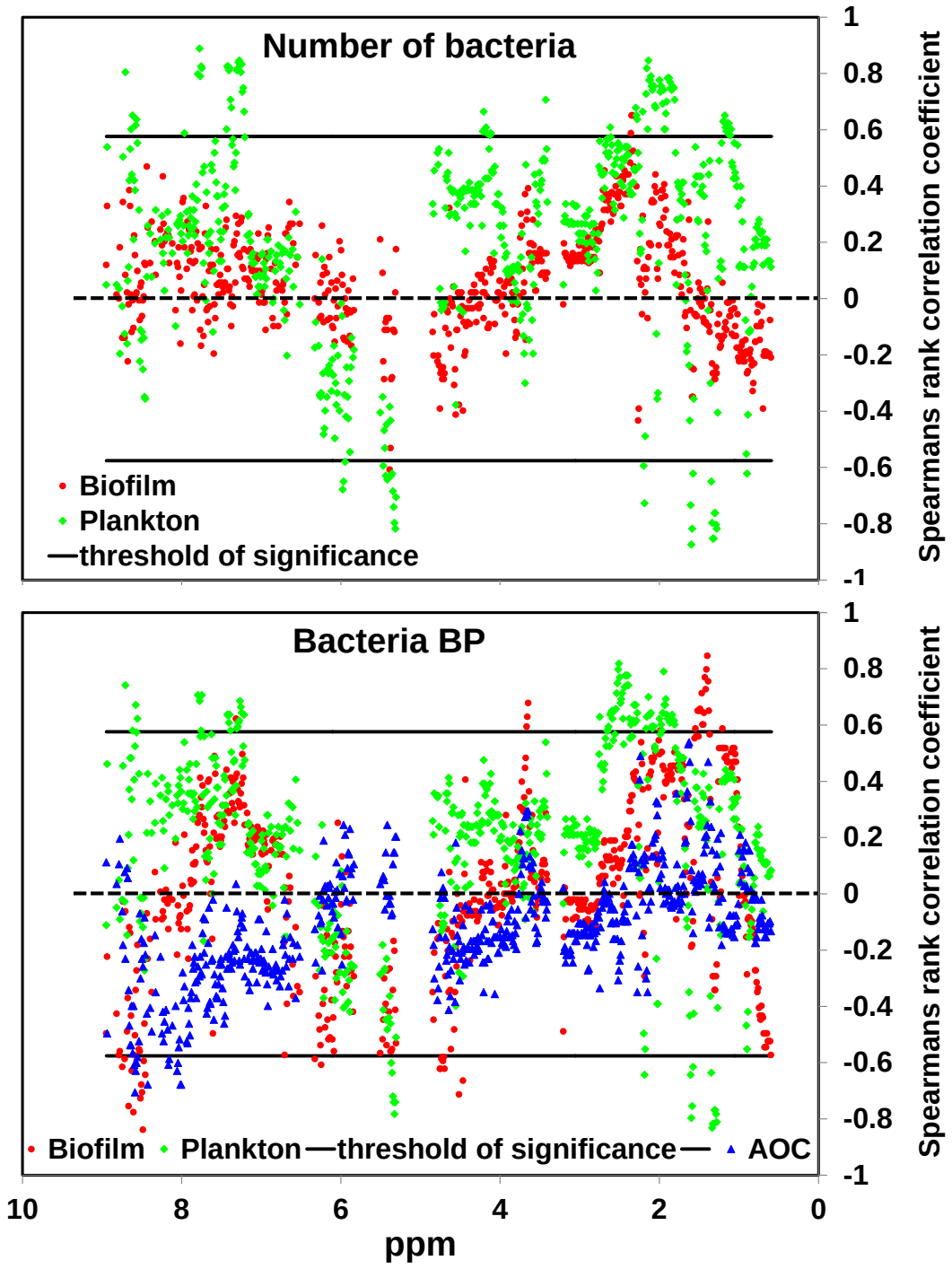
745

746 Fig. 8: Significance levels of the rank correlations between FTICR MS components present in
747 all samples and bacterial abundance, bacterial production and assimilable organic carbon.



748

749 Fig. 9: Rank correlation coefficients between ^{1}H NMR section integrals (0.01 ppm) and
750 bacterial abundance, bacterial production and assimilable organic carbon (coeffitions <-0.576
751 and >0.576 are significant at p<0.05).



752